JOURNAL OF AIRCRAFT
Vol. 41, No. 2, March–April 2004

Elastic Analysis of a Pin-Loaded Lug

A. Aslam*
Mepco Schlenk Engineering College, Tamil Nadu 626 005, India
and
G. S. Sekhon† and R. Kumar‡
Indian Institute of Technology Delhi, New Delhi 110 016, India

A numerical study is described of the elastic deformation of a pin-loaded lug. A boundary element model for engineering analysis of elastic deformation of the round ended lug is proposed. Computational results on the deformation pattern, stress distribution, effect of pin–ligament interface, influence of pin interference, effect of the ratio of lug width *W* and height of lug, *H*, to hole diameter *D* are obtained and discussed.

Introduction

THE lug is a subject matter of the proposed study. It is used in structures, load-lifting and load-carrying systems, and machinery and because it is also used in aircraft structures, its study has attracted serious and often classified research attention. In situations where loads are to be temporarily attached on to a stationary or moving structure, lug joints are often used. Lug joints are commonly used for load transfer between two structural components. The basic configuration of lug is a hole fitted with a pin, as shown in Fig. 1. The lug allows relative movement and permits easy installation and dismantling. In certain applications, for example, aircraft structures, careful design of a lug is of utmost importance because consequences of its failure can be very severe. Increasingly sophisticated methods are being employed for investigating the distribution of stress and strain in the body of the lug.

To this end, various experimental, analytical, and numerical techniques have been employed. For example, Schijve and Hoeymakers,[1] following the procedure developed by James and Anderson,[2] obtained empirical stress intensity factor relations from the crack growth rate data of through-the-thickness cracks under constant-amplitude loading. Nicoletto and Gianni[3] on the other hand, used the frozen stress photoelasticity method to determine approximate stress intensity factor solutions for both through-the-thickness and corner cracks in those components. Jessop et al.[4,5] also conducted photoelasticity experiments and obtained stress distribution in araldite plates incorporating an interference fit rigid pin. Cox and Brown[6] found that, in an uncracked lug, the stress concentration at the point of minimum cross section is relatively insensitive to pin clearance. Heywood[7] studied the effect of friction at the pin–lug interface on stresses in a lug. A photoelastic model fitted with an interference-fit duralumin pin was tested. He found that the influence of pin clearance on the stress concentration factor in the lug is rather anomalous. Gencoz et al.[8] obtained the distribution of pin bearing pressure from photoelastic test data. Fatigue crack growth tests on aluminum, titanium, and steel lugs were used to compare the stress intensity factor solutions. Stress intensity factor distributions from crack growth measurements in lugs were obtained by Moon.[9] Cartwright and Ratcliffe[10] carried out experiments on an Instron machine to determine the strain energy release rate in the case of two equal radial cracks emanating from a central hole in a finite width strip. The load was transmitted to the strip through a neatly fitting pin in the central hole. The stress intensity factor was calculated in terms of the compliance derivative.[11] Analytically, a relatively simple compounding method, which involves the superposition of known solutions, was applied to cracks in lugs by Krikby and Rooke[12] and by Liu and Kan.[13]

More recently, years, numerical methods have become quick and expedient means of treating lug problems. In this regard, the finite element method hitherto had been the computational technique used almost exclusively for investigating this type of problem. Examples include the work of Pian et al,[14] Wang,[15] and Kathiresan et al.[16] Pian et al.[14] analyzed the pin-loaded lug problem by assuming the pin loading to be either uniform or varying according to a cosine stress function. Wang[15] used the general purpose finite element code ABAQUS for the stress analysis of a round-ended lug. Computational results showed that the peak stress in the lug is rather sensitive to the magnitude of the transmitted load and the clearance of the fit between the pin and the lug. Kathiresan et al.[16] proposed an approach based on finite elements, Green's function, and correlation factors for the prediction of stress intensity factors for corner cracks in attachment lugs. Satishkumar et al.[17] studied the case of a cracked lug fitted with an oversized pin and developed a finite element contact algorithm to deal with dynamic contact at the pin–plate interface using direct iterations and a marching scheme.

An alternative computational technique, which has gained much prominence in recent years in engineering stress analysis, is the boundary element method. It is increasingly being used for this type of problem, for example, Refs. 18 and 19, although reports of its use in this area remain fairly limited in number. The key attractiveness of this method lies in that only the boundaries of the solution domain need to be modeled. Man et al.[20] analyzed the pin lug problem by discretizing them separately and setting up continuity and compatibility equations at the contacting node pairs in the form of constraints.

For the elastic analysis of the lug, the boundary element method offers distinct advantages over the finite element method. The former considers both displacement and tractions as primary unknowns, which may be independently represented with an equal degree of accuracy. In particular, the coupling of normal and tangential tractions can be handled with ease. Also, the contact pressure between the pin and the ligament can be obtained directly. In fact, the boundary element technique has emerged as an efficient numerical tool for solving problems involving steep stress gradients, such as those occurring in a cracked lug. The authors developed an efficient and robust elastic boundary element model for the analysis of stress in a lug and obtained detailed computational results to help the lug designer.

Proposed Model

The ligament is considered as a homogeneous elastic body of uniform thickness. Otherwise, the ligament geometry can be arbitrary.

Presented as Paper 2002-1325 at the AIAA/ASME/ASCE/AHS/ASC 43rd Structures, Structural Dynamics, and Materials Conference, Denver, CO, 22 April 2002; received 25 November 2002; revision received 5 May 2003; accepted for publication 12 June 2003.

*Assistant Professor, Department of Civil Engineering, Sivakasi.
†Professor, Department of Applied Mechanics.
‡Chief Design Engineer, Instrument Design Development Centre.

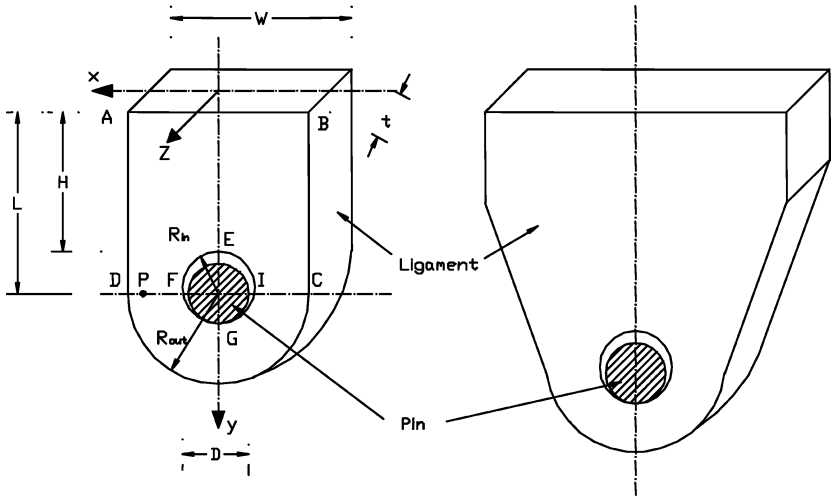

Fig. 1 Typical lug configuration.

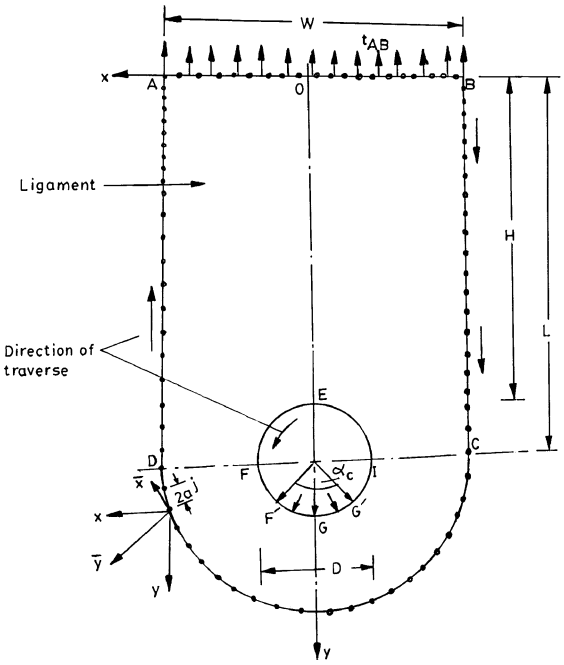

Fig. 2 Proposed boundary element model.

The height and width of the ligament are assumed to be much larger than its thickness. The coordinate system is chosen so that the z axis lies in the thickness direction (Fig. 2). A pin made of a rigid material passes through a hole in the ligament. During the loading process, the pin is assumed to remain stationary. An upward load is gradually applied at the top end of the ligament. The length of the contact between the rigid pin and the ligament along the hole boundary is assumed to be known a priori. The nature of friction at the pin ligament interface is also considered to be given. Radial cracks emanating from points on the hole boundary may or may not be present.

Governing Equations

Kelvin's solution (see Ref. 21) for a line load acting in the interior of an infinite elastic medium can be used to derive expressions for the components of displacement and stress at any point in the elastic medium. It can be shown that if p_s^j and p_n^j are the tangential and normal stress components on the jth boundary element, displacements u and v in the x and y directions at any point (x, y) are obtained as follows:

$$u = U_s P_s^j + U_n P_n^j, \qquad v = v_s P_s^j + v_n P_n^j \tag{1}$$

where U_s, U_n, v_s, and v_n are influence coefficients. (The derivation for the influence coefficients is rather lengthy and is omitted to conserve space, Interested readers may find them in Ref. 22). Similarly, the components of stress σ_x, σ_y, and τ_{xy} in the elastic medium are related to the components of applied stress p_s^j and p_n^j and are given by the following equations:

$$\sigma_x = s_{xs} p_s^j + s_{xn} p_n^j, \qquad \sigma_y = s_{ys} p_s^j + s_{yn} p_n^j$$

$$\tau_{xy} = s_{xys} p_s^j + s_{xyn} p_n^j \tag{2}$$

where expressions for s_{xs}, s_{xn}, s_{ys}, s_{yn}, s_{xys}, and s_{xyn} are influence coefficients. Specifying the point to the center of the ith element and summing the effects of applied stresses on all of the N elements, $j = 1, \ldots, N$, we get the following equations for tangential and normal components of displacements δ_s^i and δ_n^i and tangential and normal stress components τ_s^i and τ_n^i at the midpoint of the ith element:

$$\delta_s^i = \sum_{j=1}^{N} A_{ss}^{ij} p_s^j + \sum_{j=1}^{N} A_{sn}^{ij} p_n^j$$

$$\delta_n^i = \sum_{j=1}^{N} A_{ns}^{ij} p_s^j + \sum_{j=1}^{N} A_{nn}^{ij} p_n^j \tag{3}$$

$$\tau_s^i = \sum_{j=1}^{N} B_{ss}^{ij} p_s^j + \sum_{j=1}^{N} B_{sn}^{ij} p_n^j$$

$$\tau_n^i = \sum_{j=1}^{N} B_{ns}^{ij} p_s^j + \sum_{j=1}^{N} B_{nn}^{ij} p_n^j \tag{4}$$

where A_{ss}^{ij}, A_{sn}^{ij}, A_{ns}^{ij}, and A_{nn}^{ij} are influence coefficients for displacement and B_{ss}^{ij}, B_{sn}^{ij}, B_{ns}^{ij}, and B_{nn}^{ij} are the influence coefficients for stress.[22] Note that both the displacement and the stress influence coefficients depend on mechanical properties of the elastic medium and the lengths and orientations of individual boundary elements of the body.

Solution Technique

In the governing equations (3) and (4), there are $2N$ fictitious stress components p_s^j and p_n^j, j varying $1, 2, \ldots, N$. Therefore, we obtain a system of $2N$ linear simultaneous algebraic equations having as many unknowns. In the proposed model for the analysis of a lug, four types of boundary conditions exit: 1) on a set of M_1 elements, where both the stress components are prescribed, 2) a set

of M_2 elements, where both the displacement components are prescribed, 3) M_3 elements, where the tangential stress component τ_s and normal displacement δ_n are prescribed, and finally 4) M_4 elements, functional relationship between tangential and normal stress components of stress σ_n and σ_s, that is, coefficient of friction, and normal displacement δ_n is obviously prescribed,

$$N = M_1 + M_2 + M_3 + M_4 \tag{5}$$

Corresponding to the set of M_1 elements, we have a set of two M_1 equations represented by

$$(\tau_s)_i = \sum_{j=1}^{N} B_{ss}^{ij} p_s^j + \sum_{j=1}^{N} B_{sn}^{ij} p_n^j$$

$$(\tau_n)_i = \sum_{j=1}^{N} B_{ns}^{ij} p_s^j + \sum_{j=1}^{N} B_{nn}^{ij} p_n^j \tag{6}$$

where i refers to elements in set 1.

In the case of the second set of M_2 elements, we obtain the following conditions:

$$\left(\delta_s^k\right) = \sum_{j=1}^{N} A_{ss}^{kj} p_s^j + \sum_{j=1}^{N} A_{sn}^{kj} p_n^j$$

$$\left(\delta_n^k\right) = \sum_{j=1}^{N} A_{ns}^{kj} p_s^j + \sum_{j=1}^{N} A_{nn}^{kj} p_n^j \tag{7}$$

where k belongs to the set M_2, The two M_3 equations pertaining to the third set of elements may be written as

$$\left(\tau_s^l\right) = \sum_{j=1}^{N} B_{ss}^{ij} p_s^j + \sum_{j=1}^{N} B_{sn}^{ij} p_n^j$$

$$\left(\delta_n^l\right) = \sum_{j=1}^{N} A_{ns}^{ij} p_s^j + \sum_{j=1}^{N} A_{nn}^{ij} p_n^j \tag{8}$$

where l belongs to the set M_3. Last, the two M_4 conditions corresponding to the fourth set of elements are given by

$$\sum_{j=1}^{N} B_{ss}^{ij} p_s^j + \sum_{j=1}^{N} B_{sn}^{ij} p_n^j = -\mu \sum_{j=1}^{N_{ns}^{mj}} p_s^j + \sum_{j=1}^{N} B_{nn}^{mj} p_n^j$$

$$\left(\delta_n^m\right)_0 = \sum_{j=1}^{N} A_{ns}^{mj} p_s^j + \sum_{j=1}^{N} A_{nn}^{mj} p_n^j \tag{9}$$

where m belongs to the set M_4 and m is the coefficient of friction at the interface between the pin and ligament. Equations (6–9) constituting the system of equations may be collected as follows:

$$[C]\{P\} = \{B\} \tag{10}$$

where $[C]$ is a $2N \times 2N$ matrix of appropriate influence coefficients, $\{P\}$ is a $2N \times 1$ column matrix of unknown fictitious stresses, and $\{B\}$ is a $2N \times 1$ column matrix of prescribed boundary displacement or stresses. The solution of the preceding system of equations yields values of fictitious stresses p_s^j and p_n^j, $j = 1, 2, \ldots, N$. These values may then be substituted in Eqs. (1) and (2) to obtain stress and displacements at any desired point within the problem domain.

The model just discussed represents a plane stress problem of the theory of elasticity. Because the geometry is arbitrary, the solution can be achieved only through numerical means. In the present study, the boundary element method has been used for analyzing the model.

Boundary Element Code

A special purpose boundary element code has been developed for solving the proposed model. It is applicable to plane stress problems. The formulation and numerical procedure described in the foregoing paragraphs are implemented in the program. The program BEM2D comprises the following segments:

1) The main segment reads file containing information about the lug geometry, the material parameters, and the number of elements on each boundary segment. It also calls the different subroutines in an appropriate order.

2) The subroutine profile automatically generates the desired number of elements on each boundary segment and computes their orientations relative to the global coordinates.

3) The purpose of the subroutine contact is to apply the boundary conditions on the elements defining the pin–ligament interface.

4) Subroutine internal points (intpts) generate coordinates of points of interest within the lug boundary where it is desired to compute the components of stress and deformation.

5) The subroutine coefficient generates the coefficients given in Eqs. (1).

6) The subroutine influence computes different influence coefficients for deflections and stresses given in Eqs. (3).

7) The subroutine solve is used for the solutions of system Eqs. (10).

8) The subroutine bound computes the components of stress and displacement at each boundary element.

9) The subroutine stress is used for computing stress and displacement components at internal points of interest.

Computational Results

To obtain the computational results, a round ended aluminium lug (Fig. 2) having the following dimensions was considered: $L = 162.5$ mm, $W = 75$ mm, $D = 25$ mm, and $H = 150$ mm. The thickness of the lug was taken to be 12.5 mm. Analysis of the tensile test data on aluminium specimens guided the following values of the material parameters: $E = 70{,}000$ N/mm^2 and $\nu = 0.33$. The normal stress t_{AB} on the boundary AB was taken as 10 N/mm^2. The diameter of pin was considered to be equal to the hole diameter so that, when loaded, the contact length extended over whole of the lower half-circumference of the hole, resulting in an angle of contact $\alpha_c = 180$ deg. Sticking friction was assumed over the length of pin ligament contact. The boundary AB of the lug was divided into 20 elements of equal length, boundaries BC and DA into 10 elements each, and boundary CD into 20 elements. The hole boundary EFF′GG′IE of the structurally integral lug was divided into 36 equal size elements.

For the sake of generality, the different components of stress have been nondimensionalized by dividing each by a so-called nominal stress σ_{nom} defined as follows:

$$\sigma_{\mathrm{nom}} = \frac{t_{\mathrm{AB}} \times \mathrm{AB}}{2\mathrm{FD}} \tag{11}$$

where the lengths AB and FD are as shown in Fig. 2. The components of displacement have been divided by the hole diameter to render them non-dimensional. (All nondimensionalized quantities carry a superscript asterisk). The distance ξ of any point P from F has been nondimensionalized as follows:

$$\xi^x = \xi/\mathrm{FD} \tag{12}$$

where

$$\mathrm{FD} = (W - D)/2 \tag{13}$$

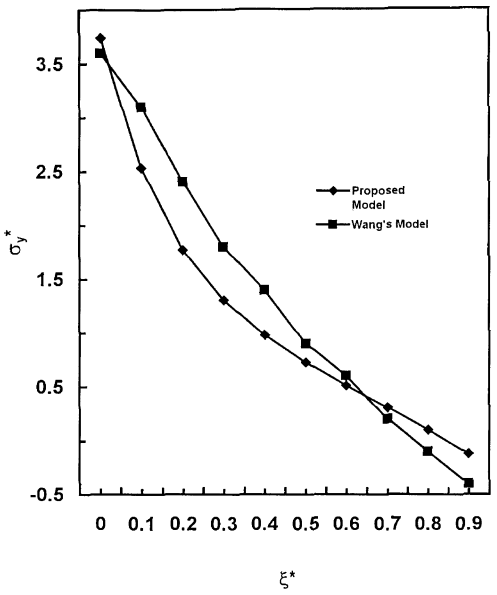

Fig. 3 Variation of σ_y^* with nondimensionalized horizontal distance ξ^* (point load case).

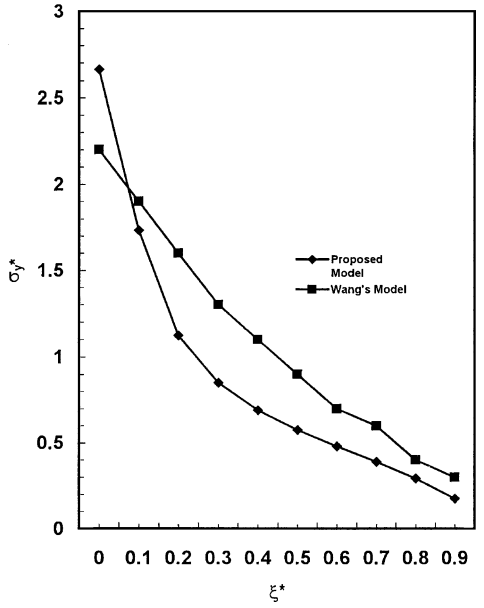

Fig. 4 Variation of σ_y^* with nondimensionalized horizontal distance ξ^* (push fit case).

Verification of Proposed Model

The predictions of the proposed model were compared with those of a corresponding finite element model by Wang.[15] Figures 3 and 4 show a comparison of the variation of σ_y^* and distance ξ^*. The present results are approximately same as those of Wang. However, the stress concentration factors predicted by the present boundary element model are higher (and, therefore, more conservative) than those reported by Wang. This can be attributed to the fact that the predictions of a finite element model are usually less accurate than those of a corresponding boundary element model, especially in situations involving high stress gradients.

Deformation Pattern

Figure 5 shows the resultant displacement at different points of the ligament as a result of a uniform upward traction acting at the top end AOB of the ligament and point contact condition prevailing at point G (Fig. 2). The displacements in Fig. 5 have been magnified by 50 times to make them observable. The maximum nondimensionalized resultant displacement δ^* is found to be 8.36×10^{-4}.

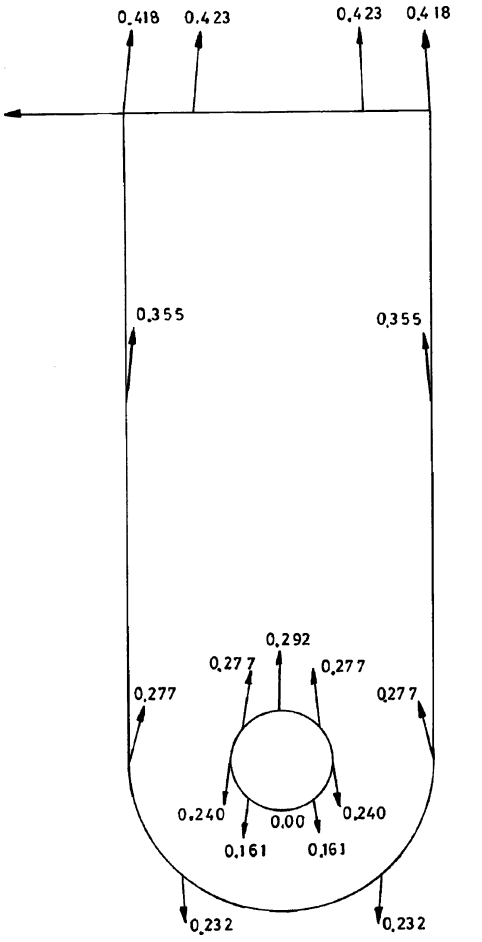

Fig. 5 Resultant displacement at key points of the lug.

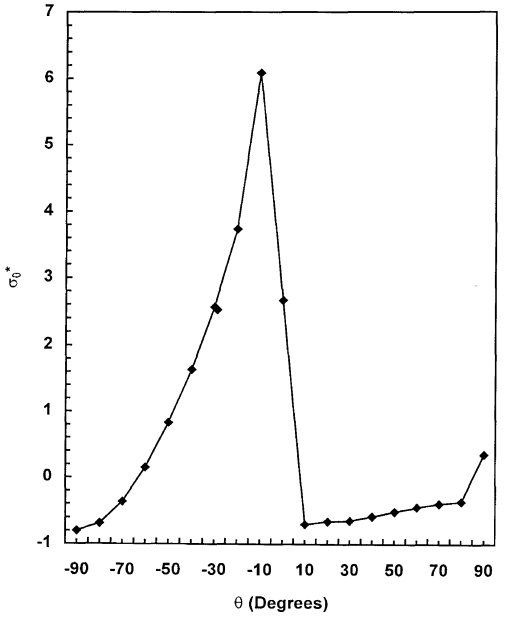

Fig. 6 Variation of σ_θ^* with θ at $r = D/2$ (push fit case).

Distribution of Stresses on Hole Boundary

Stress distribution along the hole boundary is of special interest. The variation of hoop stress σ_θ^* with angle θ at $r = D/2$ is shown in Fig. 6. Here, σ_θ^* rises as θ increases from -90 deg and attains a maximum at $\theta = 10$ deg. In the range $-10 < \theta < 10$ deg, σ_θ^* decreases rapidly. There is a slight increase in σ_θ^* as θ increases from 10 to 90 deg. Observe that the maximum value 6.08 of the hoop stress occurs at $\theta = -10$ deg. This is in close agreement with the finding

of Frocht and Hill[23] based on their photoelastic study of the lug that maximum hoop stress occurs at a value of 9 deg, that is, 81 deg anticlockwise of point E (Fig. 2). The largest principal stress σ_1^*, of course, is identical to that of the hoop stress σ_θ on the unloaded portion of the boundary. However, on the loaded portion, the pattern of the variation with angle θ is different, as shown in Fig. 7. It is found that σ_1^* increases rapidly in the range $-70 < \theta < -10$ deg and attains a maximum value of 6.08 at $\theta = -10$ deg. Between $\theta = -10$ and $\theta = 10$ deg, it decreases rather rapidly. Thereafter, the decrease is very gradual. At $\theta = 0$ deg, the value of the principal stress σ_1^* is 5.44, which is somewhat smaller than the maximum value of 6.08.

Effect of Contact Length

The contact length primarily depends on the nature of the fit. An increase in clearance between the pin and lug decreases the angle of contact. To an extent, the magnitude of the load transmitted by the rigid pin also affects the angle of contact. Increasing the external load tends to increase the angle of contact.

The effect of the contact angle on the distribution of stress σ_y^* on the horizontal plane passing through the hole boundary is shown in Fig. 8. It is found that, for $\alpha_c > 60$ deg, there is hardly any change in

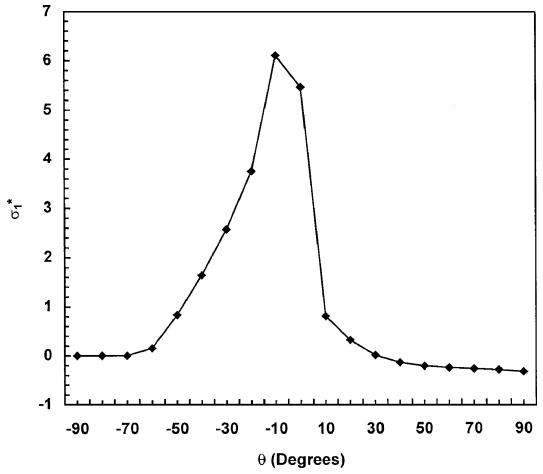

Fig. 7 Variation of nondimensionalized maximum principal stress σ_y^* with θ at $r = D/2$ (push fit case).

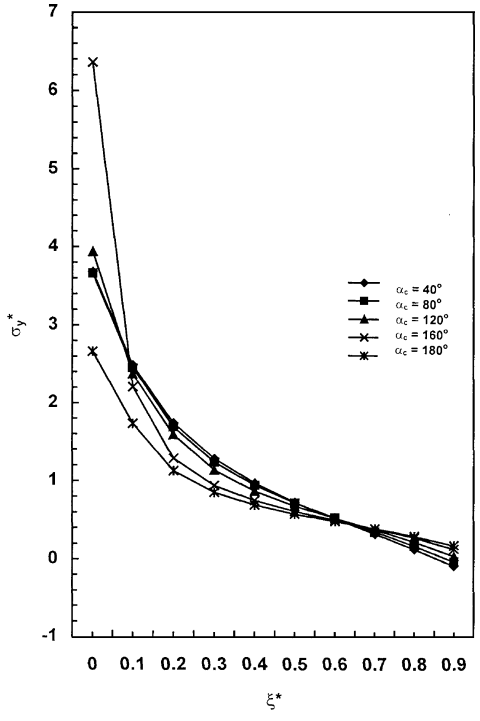

Fig. 8 Variation of σ_y^* with contact angle α_c.

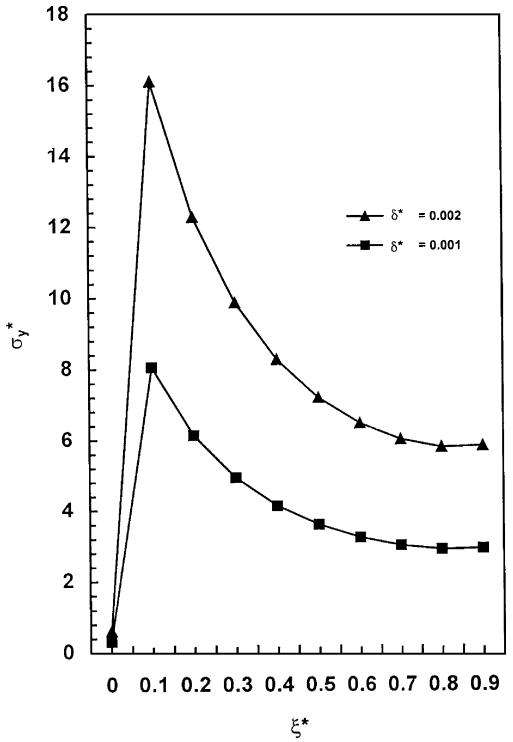

Fig. 9 Variation of σ_y^* with ξ^* due to interference alone.

the distribution of σ_y^* as a result of changes in α_c. However only for $\alpha_c = 160$ deg, there is a change in the distribution of σ_y^*. This is in general agreement with the statement of Cox and Brown[6] that, for an uncracked lug, the stress concentration at the point of minimum cross section is relatively insensitive to pin clearance. For a given external load, the maximum value of σ_y^* on the horizontal section FD (Fig. 2) is found to decrease and the smallest value to increase as the contact angle increases.

Effect of Interference

In case the pin diameter exceeds the hole diameter, for example, by an amount δ, interference conditions prevail. Furthermore, if the lug is unloaded, the contact between the pin and the ligament occurs over the whole circumference of the hole. In other words, the angle of contact becomes equal to 360 deg. Figure 9 shows the variation of σ_y^* on the line FD (Fig. 2) caused by an interfering pin in an otherwise unloaded lug. The δ^* in Fig. 9 is defined as follows:

$$\delta^* = \delta/\mathrm{D}$$

For $\delta^* = 0.002$, the maximum value of σ_y^* is found to be 16.09 and to occur at ξ^* approximately equal to 0.15. The trend of the variation of σ_y^* with ξ^* is in agreement with findings of Wanlin.[24] Beyond the point of maxima, σ_y^* decreases continuously outward toward point D.

Suppose now an external load is applied to the end AOB of the ligament (Fig. 2). The combined effect of pin interference and external load may be obtained by superposing the two effects caused by the interfering pin. Figure 10 shows the variation of σ_y^* with horizontal distance ξ^* for different values of $\delta^* = 0.002$ and 0.001. It is found that interference causes a significant increase in the stress concentration factor.

Effect of Geometrical Parameters of Ligament

The two design parameters of interest concerning the lug geometry are the ratio of the ligament width to hole diameter ratio (W/D) and the ratio of the ligament height and hole diameter (H/D). Computational results were obtained corresponding to the following values of W/D and H/D: $W/D = 3.0$, 2.5, 2.0, and 1.5, and $H/D = 6.0$, 4.0, and 2.0.

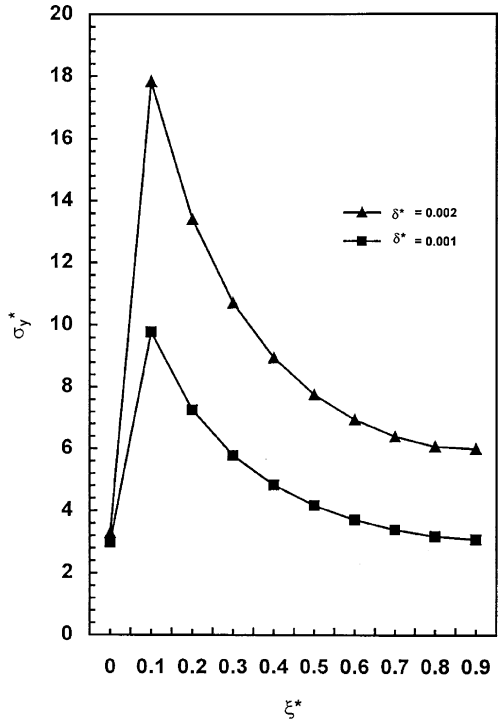

Fig. 10 Combined effect of pin interference and external load on the variation of σ_y^* with ξ^*.

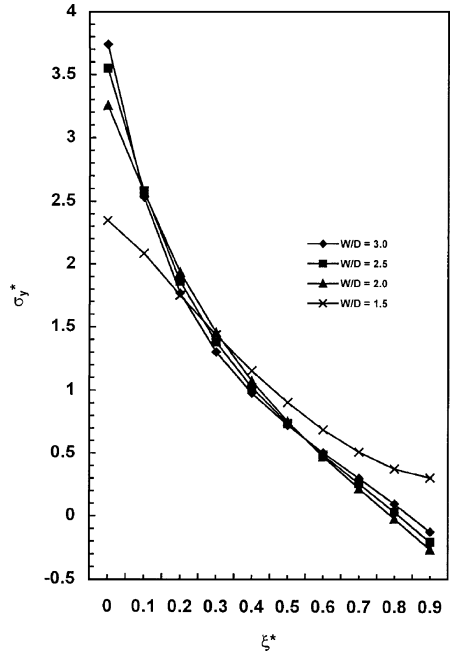

Fig. 11 Variation of σ_y^* with nondimensionalized horizontal distance ξ^* corresponding to different ratios of W/D (point load case).

Two different contact conditions, namely, point contact and contact over half the circumference, were considered. Figures 11 and 12 show the variation of σ_y^* with ξ^* corresponding to different ratios of W/D. The variations are approximately identical except for the smallest value of ratio W/D, namely, 1.5. In the last case, the peak stress σ_y^* is found to be significantly lower.

Variation of σ_y^* with ξ^* corresponding to different ratios of H/D and the mentioned two contact conditions are given in Table 1. It is observed that the ratio H/D does not materially affect the peak stress σ_y^*. This observation is in agreement with the findings of Liu and Tan[19] that the peak stress $(\sigma_y^*)_{\max}$ remains virtually unchanged with changes in the values of the parameter H/D.

Table 1 Variation of σ_y^* with nondimensionalized horizontal ξ^*

ξ^*	σ_y^* (point load)	σ_y^* (push fit condition)
	H/D ratio = 2.0	
0.1	2.5887	1.7436
0.2	1.8068	1.1315
0.3	1.33	0.8565
0.4	0.9976	0.6951
0.5	0.7379	0.58
0.6	0.5138	0.484
0.7	0.3035	0.393
0.8	0.0908	0.2983
0.9	−0.1397	0.1934
	H/D ratio = 4.0	
0.1	2.5524	1.7364
0.2	1.7843	1.1259
0.3	1.3158	0.8526
0.4	0.9894	0.6925
0.5	0.7345	0.5787
0.6	0.5147	0.4838
0.7	0.3085	0.3934
0.8	0.1005	0.2978
0.9	−0.1247	0.1865
	H/D ratio = 6.0	
0.1	2.5308	1.7326
0.2	1.7696	1.1232
0.3	1.3047	0.8504
0.4	0.9805	0.6907
0.5	0.7272	0.577
0.6	0.509	0.4818
0.7	0.3052	0.3906
0.8	0.1011	0.2926
0.9	−0.1188	0.1752

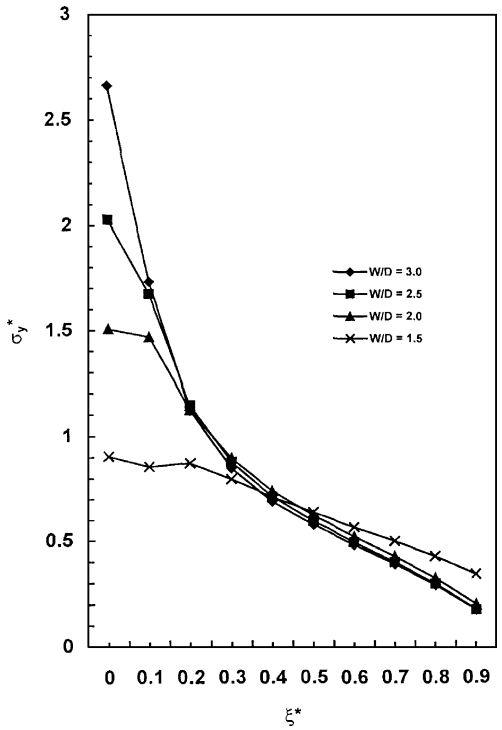

Fig. 12 Variation of σ_y^* with nondimensionalized horizontal distance ξ^* corresponding to different ratios of W/D (push fit case).

Conclusions

A two-dimensional boundary element model has been proposed for engineering analysis of elastic deformation of a lug of arbitrary shape subjected to arbitrary loads. It is assumed that the length of contact between the pin and the ligament is known a priori. A computational procedure and a corresponding special purpose FORTRAN program have been developed to set up and solve the system

equations. The program is robust and computationally efficient. Predicted values of stress have been compared with published results. Detailed computational results have been obtained and analyzed.

References

[1]Schijve, J., and Hoeymakers, A. H. W., "Fatigue Crack Growth in Lugs and the Stress Intestity Factors," Univ. of Technology, Rept. LR 273, Delft, The Netherlands, July 1978.

[2]James, L. A., and Anderson, W. E., "A Simple Experimental Procedure for Stress Intestity Calibrations," Engineering Fracture Mechanics, Vol. 1, 1969, pp. 565–568.

[3]Nicoletto, G., and Gianni, N., "Experimental Characterization of Crack at Straight Attachment Lugs," Engineering Fracture Mechanics, Vol. 22, March 1985, pp. 829–838.

[4]Jessop, H. T., Snell, C., and Holister, G. S., "Photoelastic Investigation on Plates with Single Interference-Fit Pins with Loading Applied to Plate Only," Aeronautical Quarterly, Vol. 7, 1956, pp. 297–314.

[5]Jessop, H. T., Snell, C., and Holister, G. S., "Photoelastic Investigation on Plates with Load Applied (a) to Pin Only and (b) to Pin and Plate Simultaneously," Aeronautical Quarterly, Vol. 9, 1958, pp. 147–163.

[6]Cox, H. L., and Brown, A. F. C., "Stress Around Pins in Holes," Aeronautical Quarterly, Vol. 15, 1963, pp. 357–372.

[7]Heywood, R. B., *Designing by Photo-Elasticity*, Chapman and Hall, London, 1952.

[8]Gencoz, O., Goranson, U. G., and Merril, R. R., "Application of Finite Element Techniques for Predicting Crack Propagation in Lugs," *International Journal of Fatigue*, 1980, pp. 121–129.

[9]Moon, J. E., "The Effect of Frictional Forces on Fatigue Crack Growth in Lugs," *Proceedings of the 12th ICAF Symposium*, Vol. 1.6, Toulouse, 1983, pp. 1–53.

[10]Cartwright, D. J., and Ratcliffe, G. A., "Strain Energy Release Rate for Radial Cracks Emanating from a Pin Loaded Hole," *International Journal of fracture Mechanics*, Vol. 8, No. 2, 1972, pp. 175–181.

[11]Irwin, G. R., and Kies, J. A., "Critical Energy Rate Analysis of Fracture Strength," *Welding Research Supplement*, April 1954.

[12]Krikby, W. T., and Rooke, D. P., "A Fracture Mechanics Study of Residual Strength of Pin–Lug Specimens," *Fracture Mechanics in Engineering Practice*, edited by P. Stanley, Applied Scientific, London, 1977, pp. 339–360.

[13]Liu, A. F., and Kan, H. P., "Test and Analysis of Cracked Lugs," *Fracture 1977*, edited by D. M. R. Taplin, ICF4, Vol. 3, Waterloo, Canada, 1977, pp. 657–664.

[14]Pian, T. H. H., Mar, J. W., Orringer, O., and Stalk, G., "Numerical Computation of Stress Intensity Factors for Aircraft Structural Details by Finite Element Method," U.S. Air Force Flight Dynamics Lab., Rept. AFFDL-TR-76-12 Wright–Patterson AFB, OH, May 1976.

[15]Wang, G. S., "Stress Analysis for a Lug Under Various Conditions," *Journal of strain analysis*, Vol. 29, No. 1, 1994, pp. 7–16.

[16]Kathiresan, K., Brussat, T. R., and Rudd, J. L., "Crack Growth Analysis and Correlation for Attachment Lugs," *Journal of Aircraft*, Vol. 22, No. 9, 1985, pp. 818–824.

[17]Satishkumar, K., Dattaguru, B., and Ramamurthy, T. S., "Analysis of a Cracked Lug Loaded by an Interference Fit Pin," *Int. J. Mech. Sci.*, Vol. 38, No. 8-9, 1996, pp. 967–979.

[18]Chen, W. H., and Chen, T. C., "Boundary Element Analysis of Contact Problems with Friction," *Computers and Structures*, Vol. 45, 1992, pp. 431–438.

[19]Liu, S. B., and Tan, C. L., "Boundary Element Analysis of Contact Problems with Friction," *Computers and structures*, Vol. 53, No. 3, 1994, pp. 653–665.

[20]Man, K. W., Alliabadi, M. H., and Rooke, D. P., "Stress Intensity Factors in the Presence of Contact Stresses," *Engineering Fracture Mechanics*, Vol. 51, No. 4, 1995, pp. 591–601.

[21]Timoshenko, S. P., and Goodier, J. N., *Theory of Elasticity*, McGraw–Hill, New York, 1970.

[22]Crouch, S. L., and Starfield, A. M., "Boundary Element Methods in Solid Mechanics," George Allen and Urwin, London, 1983.

[23]Frocht, M. M., and Hill, H. N., "Stress Concentration Factors Around a Central Circular Hole in a Plate Loaded Through Pin a Hole," *Journal of applied mechanics*, Vol. 7, No. 62, 1940, pp. 62-A5–A9.

[24]Wanlin, G., "Elastic-Plastic Analysis of a Finite Sheet with a Cold-Worked Hole," *Engineering Fracture Mechanics*, Vol. 45, No. 6, 1993, pp. 857–864.